Available online at www.sciencedirect.com
SCIENCE DIRECT®

Journal of the European Ceramic Society 24 (2004) 3187–3194

www.elsevier.com/locate/jeurceramsoc

Exfoliable organo-montmorillonite nano-fillers for polymer/ceramic composites

A. Goldstein*, M. Beer

Israel Ceramic and Silicate Institute, Technion City, 32000 Haifa, Israel

Received 28 August 2003; received in revised form 9 November 2003; accepted 15 November 2003

Abstract

The preparation of exfoliable organo-montmorillonites, usable as nano-fillers in polymer-matrix composites, was studied. Such fillers are able, when added in amounts of less than 10%, to improve dramatically the engineering properties of various polymer matrices. Here, both neutral and cationic amine molecules were inserted in the silicate's gallery. The added molecules modify the water and sodium content of the gallery and also its height. The molecules' electrical state, structure and the organics/smectite ratio in the reactor, profoundly influence the characteristics of the resulting organo-montmorillonite. It was found that long chain amines, in the ionic state, are, in contrast to the short ones, able to expand substantially the montmorillonite gallery. When present in large amounts, such amines adopt, within the gallery space, arrangements which favor a height increase. Cationic state amines, aided by exchange reactions with the gallery cations, penetrate much more easily into the gallery than do neutral molecules. Practically attractive preparation technologies may be based on the use of cationic amine molecules which allow the reproducible preparation of nano-fillers, exhibiting gallery heights of ~20–26 Å, with relative ease. Such products are stable up to 280 °C.

Keywords: Exfoliation; Mechanical properties; Nano-composites; Silicates

1. Introduction

Organic, inorganic and hybrid nano-materials—in which all or a fraction of the "building blocks" exhibit a nano-size (at least in one direction)—are being developed in order to achieve raised performance and/or new functionalities.[1–7]

Various "bottom up" or "top down" methods are used for the fabrication of such materials. For instance, by dispersing ceramic nano-particles in various metallic, glassy, ceramic or polymer matrices, significant improvement of mechanical properties was obtained, compared to coarser structure materials of similar composition, e.g.[8–12] In the case of polymer matrices, the nano-fillers examined include—among others—alumina whiskers, metal oxide precipitates, sol-gel network fragments, silica tubes and smectite platelets.[13–16]

One of the most spectacular results has been attained by dispersing montmorillonite (MM) in a nylon 6 matrix.[17] At a loading of only 4% bentonite-clay, the tensile modulus of the pristine polymer was doubled, the tensile strength raised by some 50% (without losing impact strength) and the heat deflection temperature increased by 80 °C. The gas barrier and flame retardant properties were also vastly improved.[12,16–20] The properties improvement was a consequence of the insertion of rigid ceramic platelets—having a thickness in the 1–10 nm range and aspect ratios of 100–800—into the polymer. The improved performance seems to be related to the fact that, in the case of the nano-platelets, many of the properties of the composite are determined by the special structure of the vast filler/matrix interface, while the micro and macro composites exhibit properties closer to the average of the components. The nanostructure of a polymer-matrix composite including a MM based nano-filler is shown in Fig. 1.

Ceramic nano-platelets can be obtained by exploiting the peculiar structure of the smectites, a group of 2:1 layered phyllosilicates. The structure of a representative smectite, montmorillonite, is illustrated in Fig. 2.[21] The stacks of oxide nano-layers (~1 nm thick) are separated by "galleries" in which water molecules and various

* Corresponding author. Tel.: +972-4-8222107/8; fax: +972-4-8325339.
E-mail address: goldaad@actcom.co.il (A. Goldstein).

0955-2219/$ - see front matter © 2003 Elsevier Ltd. All rights reserved.
doi:10.1016/j.jeurceramsoc.2003.11.013

cations, like Na^+, K^+, Li^+ or Ca^{2+}, are located. The cations compensate the charge (negative for most natural smectites; $\delta = 0.4$–1.2 e/Si_8O_{20} unit) existent on the oxide nano-layers, due to aliovalent substitutions for the lattice Si^{4+} and/or Al^{3+} ions. The interlayer bonds are markedly weaker than the intralayer ones, so that in very diluted aqueous suspensions the nano-layers can be completely separated.[22] In more concentrated systems, though, the basic nano-layers are agglomerated in relatively "soft" multimicron size "tactoids". For the preparation of attractive composites, the polymer chains have to penetrate in between the smectite nano-layers, and separate them (tactoid exfoliation). Therefore, if the pristine smectite (present, in practice, in relatively concentrated suspensions) is mixed with a polymer, lengthy processing—in conditions in which the tactoids are subjected to the action of strong shear forces—is needed in order to attain some measure of tactoid break up.

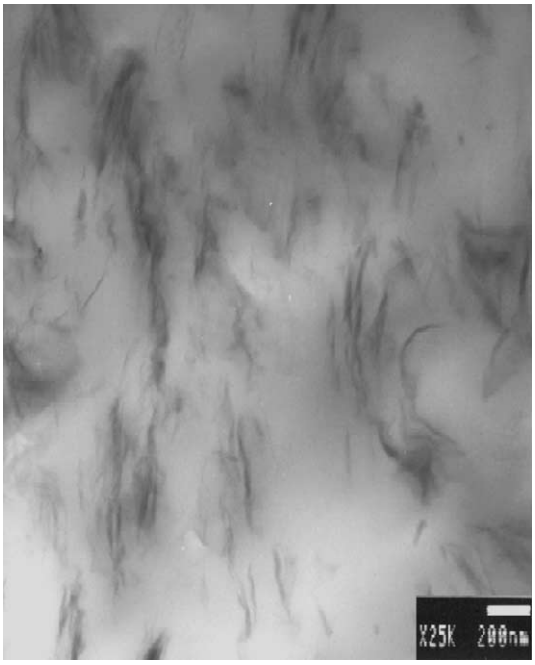

Fig. 1. Structure of polypropylene/5% organo-montmorillonite composite (fabricated by CAOL + ICSI, Haifa); TEM, bright field image showing partially and, some, fully exfoliated OM tactoids (black filaments).

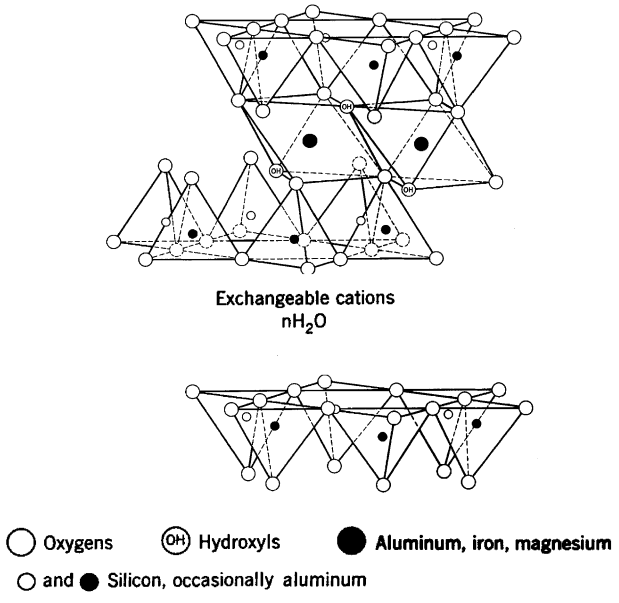

Fig. 2. Montmorillonite crystal structure[21] showing dioctahedral oxide-layers (9.5 Å), separated by gaps ("galleries").

The smectite deagglomeration process can be dramatically enhanced by suitable treatments applied prior to the contact with the polymer. One of the most efficient approaches consists in the insertion of organic molecules into the galleries of the smectite. Suitable organic gallery penetrators (OGP) act by increasing the height (H_g) of the gallery, conferring an organophilic character to the oxide surface (hydrophilic in its pristine state) and, in some cases, establishing chemical bonds with the incoming polymer matrix molecules. Insertion of the OGPs transforms the pristine MM into organo-montmorillonite (OM). If the tactoids of an OM are easily dispersed—in contact with the polymer matrix molecules—it is called an exfoliable organo-montmorillonite (EOM).

Insertion of organics into smectites—the process on which EOMs preparation is based—has been studied for a long time now.[23–27] Not all aspects—relevant for EOMs preparation—have been examined, though, and a lot of contradictory results have been published.[25,27] Therefore the development of efficient procedures for EOM preparation requires further studies.

In this work, a reference bentonite—especially well suited for gallery exchange processes—is reacted with a variety of amine based OGPs, in conditions usable in practice, for organo-montmorillonite preparation, in order to allow the identification of those able to generate EOMs exhibiting high galleries. The ability of an organo-montmorillonite to act as an EOM depends, to a large extent, on the height of its gallery.[28,29]

2. Experimental

A highly purified (97% smectite, 3% quartz) bentonite, grade PGW of Nanocor, Arlington Heights, IL, USA, was the Na enriched MM source in most of the experiments. The dry, micronized powder (specific surface area A ~ 4 m^2/g) is made up of rounded edge, variable shape, porous agglomerates with most of the particles having a size in the 5–45 μm range (Fig. 3a). The oxide layer includes various substitution ions of elements like Mg, Fe, Ti, Mn, P and S. The gallery is populated almost exclusively with Na^+ (2.8% Na content, which generates a CEC of 145 meq/100 g). Adsorbed and absorbed water content is 8–10%.

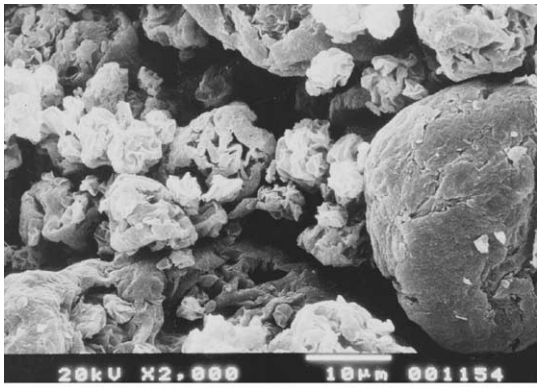

(a)

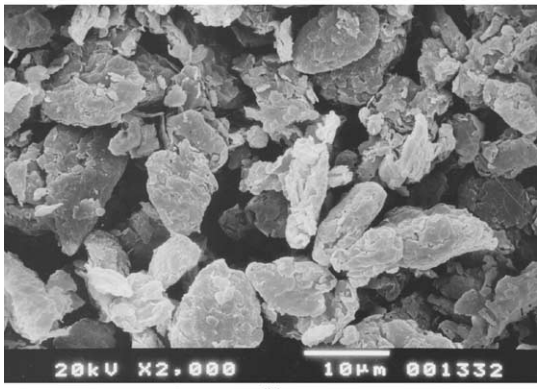

(b)

Fig. 3. Morphology, size and substructure of pristine MM particles and an ICSI prepared OM (as-dried state) SEM. (a) pristine MM, (b) OM.

The list of OGPs tested here includes: butyl (BA), nonyl (NA), octadecyl (ODA), N-methyl octadecyl (MODA), N-trimethyl octadecyl (TMODA) and N-dimethyl dioctadecyl (DMDODA) alkylammonium ions. The BA, NA and ODA were inserted in both ionic and neutral form. The chemical formulae of the alkylammonium OGPs used are listed in Table 1.

For OM synthesis, in which alkylammonium ions were the OGP, a slurry (10 g/l) was prepared by stirring the bentonite/distilled water mixture for 10–80 h at room temperature. Aqueous solutions of the OGP salt (chloride or bromide) were then added, under vigorous stirring, to the reactor at 65–90 °C. The quantitative relation between the reactants was varied in a wide range. This relation is specified in terms of the ratio between the number of gram-equivalents of OGP and gallery Na^+. This ratio was labelled R_e. The specific R_e values used are given in Tables 2–4. Rapid reaction converted the initially cream-brown color of the slurry to white. After hot vacuum filtering and several washings with alcohol/water (volumes ratio 1:1), the cake was freeze dried and milled to produce the OM powder. For OM synthesis, in which neutral molecules were used, the MM was suspended in solutions of the amine in isopropyl-alcohol (IPA) or pure liquid amine. The morphology and size of OM dry powders ($A = 3–5$ m^2/g) is illustrated in Fig. 3b.

Chemical analysis of the raw materials and OM was done by XRF (EX6500, Jordan Valley, Israel) and wet chemistry based standard silicate chemistry procedures.[30] Phase composition and gallery height were determined from XRD patterns (PW 3710, Philips). Particle morphology was visualized by SEM (JEOL SM5000), while particle size distribution was determined (suspension in ethylene glycol) with a laser scanner (CIS-1 of Galai, Israel). Powder surface area was obtained by applying the BET approximation to gas adsorption data (Quantasorb of Quantachrome). The presence of organics was ascertained from FTIR (Vector 22 of Bruker) spectra. The amount of water and organics, present within the gallery, was determined by thermogravimetry. The microstructure shown in Fig. 1, was visualized by TEM (JEOL 2000-FX).

3. Results and discussion

The main interest of this research was the development of practically usable procedures for the fabrication of EOMs exhibiting markedly expanded galleries. For this, the influence of a number of factors—on the penetration of amine within the gallery of the PGW montmorillonite and its actions there—has been examined. An important first factor was the electrical state—neutral (A°) or ionic (A^+)—of the potential OGP. The effect of other aspects, like the OGP structure and the OGP:MM ratio on the characteristics of the prepared OMs, was also studied.

Table 1
Chemical formulae of alkylamine based OGPs examined

Name	Abbreviation	Formula
Buthyl amine	BA	CH_3-$(CH_2)_3$-NH_2
Nonyl amine	NA	CH_3-$(CH_2)_8$-NH_2
Octadecyl amine	ODA	CH_3-$(CH_2)_{17}$-NH_2
N-methyl octadecyl amine	MODA	CH_3-$(CH_2)_{17}$-NH-CH_3
N-trimethyl octadecyl ammonium bromide	TMODA	CH_3-$(CH_2)_{17}$-N-$(CH_3)_3$Br
N-dimethyl dioctadecyl ammonium bromide	DMDODA	$[CH_3$-$(CH_2)_{17}]_2$-N-$(CH_3)_2$Br

Table 2
Characteristics of OMs prepared in liquids of variable polarizability ($R_e = 1.7$)

Solvent	OGP states	OGP inserted in OM [%]	Residual Na^+ and H_2O in gallery [%]		H_g [Å]
IPA (no HCl)	BA°	<1.0	2.2	10.0	3.0
IPA (HCl)	$BA^\circ + BA^+$	4.5	1.3	8.0	3.5
H_2O (HCl)	BA^+	8.5	0.6	5.0	3.5
IPA (no HCl)	ODA°	<1.0	2.5	9.0	3.0
IPA (HCl)	$ODA^+ + ODA^\circ$	18.0	0.9	5.0	11.0
H_2O (HCl)	ODA^+	39.0	0.1	1.0	26.0
H_2O	(Pristine MM)	0	2.8	10.0	3.0

Table 3
Characteristics of OMs derived from alkylammonium ions of various structure ($R_e = 1.7$) aqueous medium

A^+ type	OGP inserted [% of OM]	Residual Na^+ and H_2O in gallery [%]		H_g [Å]	OGP loss at 200 °C [%]
BA^+	8.5	0.60	5.0	3.5	0.65
ODA^+	39.0	0.10	1.0	26.0	0.50
$MODA^+$	37.0	0.10	1.0	26.5	0.40
$TMODA^+$	36.0	0.18	3.5	31.0	0.70
$DMDODA^+$	53.0	0.20	3.5	29.0	1.20
Na^+-MM (reference)	0	2.80	10.0	3.0	–

Table 4
Characteristics of OMs derived using various R_e values, from $MM + ODA^+$ mixtures

R_e	OGP inserted [% of OM]	Residual Na^+ and H_2O in gallery [%]		H_g [Å]	OGP loss at 200 °C [%]
0.32	10.0	1.70	9.0	3.5	0.5
0.65	21.0	0.70	3.0	18.0	0.8
1.10	30.0	0.15	1.0	22.0	0.5
1.70	39.0	0.10	1.0	23.0–26.0	0.5
2.20	36.0–40.0	0.10	0.9	23.0–26.0	0.8–1.2
1.10×3	49.0–58.0	0.08	1.2	28.0–31.0	3.0–5.0

3.1. Influence of OGP electrical state on OM formation

It is known that MM swelling (which implies gallery expansion) may be obtained, in principle, by the aid of both neutral and ionic organic molecules.[23–27,31–34] The penetration of organics into the gallery, is possible because various types of bonding (ionic, dipolar, hydrogen and Van der Waals) can be formed between the charged oxide surfaces and the incoming molecules. Total bonding may be, in many cases, stronger than that between the smectite, water and inorganic gallery ions. Published information on the influence of the potential OGP's electrical state on ease of penetration and the resulting intragallery structural modifications, is quite contradictory.[23–27,31–36] The experiments performed here, related to this issue, were designed so as to minimize the influence of other factors when comparison of the performance of different types of amine molecules—A° vs A^+—is done.

The desired molecular states have been obtained by the aid of suitable suspending liquids and control of H^+ content. In a first set of experiments, representative short (BA) and long (ODA) amines were suspended in liquids of variable polarizability (water, alcohols), while maintaining, in all cases, a R_e value of 1.7. For instance, using the slightly polar ($\epsilon_r = 16$) IPA, it was possible to dissolve neutral amines and create suspensions including, practically, only A° state molecules. Addition of HCl to IPA determined the formation of $A^\circ + A^+$ mixtures. The behavior of such systems suggests that an A^+ fraction may be obtained even in solvents which do not produce strong dissociation of the proton source. For a given acid content, the fraction of A^+ was further increased when substituting partially or totally IPA with the more polar ($\epsilon_r = 90$) H_2O. In the aqueous suspensions, practically only A^+ state molecules exist. The characteristics of the OMs obtained—while using the various solvents mentioned above—are listed in Table 2.

As it may be seen, when A° is the only species present in the reactor, organics do not enter the MM, so that the content of its gallery is only slightly affected. The slight reduction in Na^+ content is not related to OGP action. This is observed also when MM suspensions (without organics content) are heated. The amine to MM ratio used above is relatively low. It was also examined whether a substantial raise of the R_e—obtained while keeping preparation difficulties at reasonable levels—is instrumental in improving the OGP potential of A° molecules. This set of experiments has been executed using R_e ratios of respectively 25 (for BA°) and 30 (for ODA°). Even in the case of these, markedly more concentrated (in organic material) reaction systems, no significant amounts of amine could be inserted into the MM gallery. Only by soaking the MM in pure liquid amines did it become possible to confer OGP character to the A° molecules. Up to 7% of BA and 13% of NA were included in the OMs prepared in such a way. The amount of ODA° inserted could not be accurately determined due to processing difficulties (especially in the washing stage). All the OMs derived from MM + A° mixtures retained Na^+ and water, remaining quite hydrophilic. The H_g of the pristine MM could not be significantly raised when using A° type molecules as potential OGPs. High-gallery OMs, as in the β type MM–OGP complexes reported in[36]—where H_g values of up to 40 Å were obtained (preparation conditions not specified)—could not be prepared by the aid of the preparation procedures and conditions examined here.

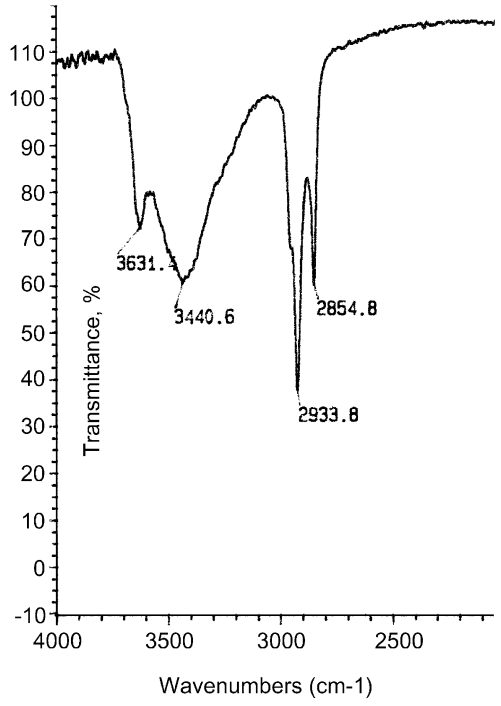

Fig. 4. Vibrational spectrum (FTIR) of an ICSI prepared OM; signals at 3631 and 3440 cm^{-1} due to respectively lattice OH^- and absorbed water; signals at 2934 and 2854 cm^{-1} due to organics (C–H system stretching vibrations).

Returning to the data in Table 2 it may be seen that—at the given $R_e = 1.7$ reactants ratio—A^+ state molecules exhibit a higher ability to act as OGPs than neutral amines. In situations where $A^+ + A^\circ$ mixtures or, better, only A^+ molecules are present, the amount of insertable amine rises drastically. In the case of the long chain ODA^+ (aqueous solvents), the incoming molecules expel both Na^+ and the water coordinated around those ions; the resulting OM has an organophilic (hydrophobic) character which is essential for a nanofiller. This only partially happens in the case of the short chain ions. When the amount of ODA^+ entering the gallery rises over about 15%, the gallery expansion becomes significant. The H_g attains a value of 11 Å in acidulated IPA, rising to an impressive 26 Å when the preparation is done in pure water.

Considering the results of Table 2, it was decided to use in all subsequent work only preparative systems based on A^+ type potential OGPs. The aqueous systems which are optimal for A^+ formation, are also the most convenient for large scale production.

3.2. OMs derived from cationic amines

The data discussed in the previous section suggest that the possibility, existent for A^+ species, to engage in ionic exchange reactions with the MM ions (Na^+ in the case of PGW), provides a very efficient mechanism for insertion of alkylammonium ions into the smectite gallery. Acid/base type reactions, possible between the hydrated Na^+ ions and the neutral R-NH_2 molecules (these exhibit base character due to the electron pair of the nitrogen atom), seem to provide a much weaker penetration mechanism, for A° type molecules. Below, various aspects related to the preparation of OMs by the aid of alkylammonium ions are examined.

3.2.1. The influence of alkylammonium ion structure

In Table 3, the characteristics of OMs, prepared using various types of A^+, are presented. It may be seen that all the A^+s penetrate massively into the smectite. The presence of organic material, in the OM, is detected by the IR spectrum, shown in Fig. 4. The two signals at ~2900 cm^{-1} are characteristic of organics (stretching vibrations of the C–H system) and are absent in the pristine MM IR spectra. The penetration yield (fraction of the amine, present in the reactor, absorbed by MM) is close to 100%. The amount of residual water and Na^+ in the OMs, are correlated between them to some extent. The ability of the alkylammonium ions to exchange for the Na^+ ions—despite entropic penalties and low cationic field strength—is quite remarkable. It seems to be due to the hydrogen bonds which the OGPs may form with the oxide surfaces. Additionally, due to the

size of the OGPs, which are larger than the Na^+ ion, the Van der Waals bonds are also significantly stronger. These types of bonding also explain the increase of exchange ability with the increase in size of the alkylammonium ion.

The structure of the A^+ has a strong influence also on the resulting OM gallery height, as the H_g values (maximal H_g values obtainable are given) in Table 3 (determined by the aid of XRD patterns like those of Fig. 5) indicate. The H_g value depends on the steric configuration adopted by the system of A^+ molecules accommodated by the gallery. Interpretation of experimental data (XRD, FTIR, NMR) and modelling of OGP/MM interactions, while not able to generate accurate detailed representations, has allowed at least a rough estimation of an OGP's steric configuration within the gallery.[24,28,29,31–37] Graphic representations of the alkylammonium ions possible orientations are given in Refs. 28,29,31. The evaluation of the intragallery configurations obtained here is based on the findings presented in the above mentioned publications. For instance, in the case of the BA^+, it is clear that the molecule lies with the plane of the zigzag carbon chains parallel to the oxide layers—despite the quite high surface charge of the PGW—so that the H_g is only ~3.5 Å, similar to that of the pristine MM. According to, Ref. 31 for smectites with high negative layer-charge surface density—like the PGW-MM used here—even such short molecules may adopt more vertical positions. In such a case, though, a H_g of ~10 Å would have been expected. The long "snake" shaped ODA^+ and $MODA^+$ adopt, when $R_e = 1.7$, a paraffin-like arrangement, with the chains almost in vertical position relative to the oxide surfaces. For OMs prepared in systems having $R_e = 1.7$, the gallery space is, in the case of the large A^+s, quite crowded, favoring vertical orientations. The quaternary "octopus" shaped TMODA and DMDODA alkylammonium ions produce the highest OM galleries, H_g~30 Å. Were the long molecules to adopt a flat orientation, the H_g values would have been smaller than 15 Å even in the case of a trilayer arrangement. Flat arrangements seem to be present in the case of the OMs prepared in acidulated IPA (Table 2) even when ODA is the OGP. The OGP content of the gallery is lower there and part of it is probably A° type. Data, not given here, strongly suggest that in systems where A^+ OGPs expand the gallery, a fraction of the coexisting A° species is also allowed in. In the case of TMODA, the XRD pattern shows an additional peak [apparently not an overtone of (001)], corresponding to a value of 26.7 Å, the significance of which is not presently understood.

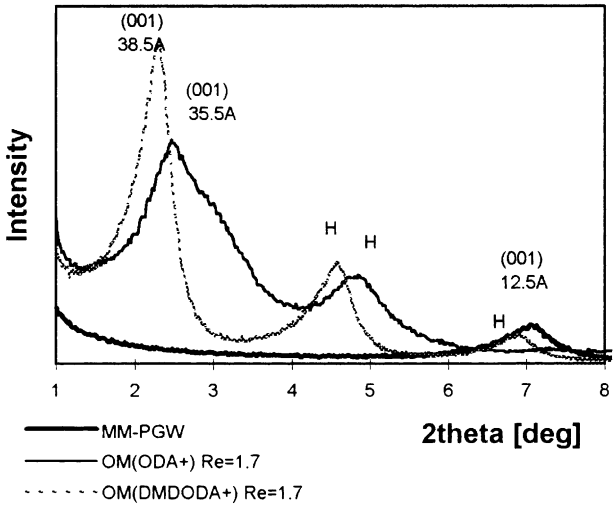

Fig. 5. XRD pattern of MM and OMs including ODA^+ and $DMDODA^+$ type OGPs. H: higher order reflections from same stack of planes that generate (001) peak; (001): reflection due to MM lattice planes that limit the gallery.

3.2.2. Thermal stability of OMs

The fabrication of polymer/OM composites may expose the nano-filler—depending on the nature of the matrix and the technology used—to temperatures in the range 100–250 °C, in some cases even higher. Due to this, it is important to examine the behavior of OMs at such temperatures.

In Fig. 6, the mass loss, on isothermal heating (1 h at each temperature) of pristine PGW-MM, free ODA and

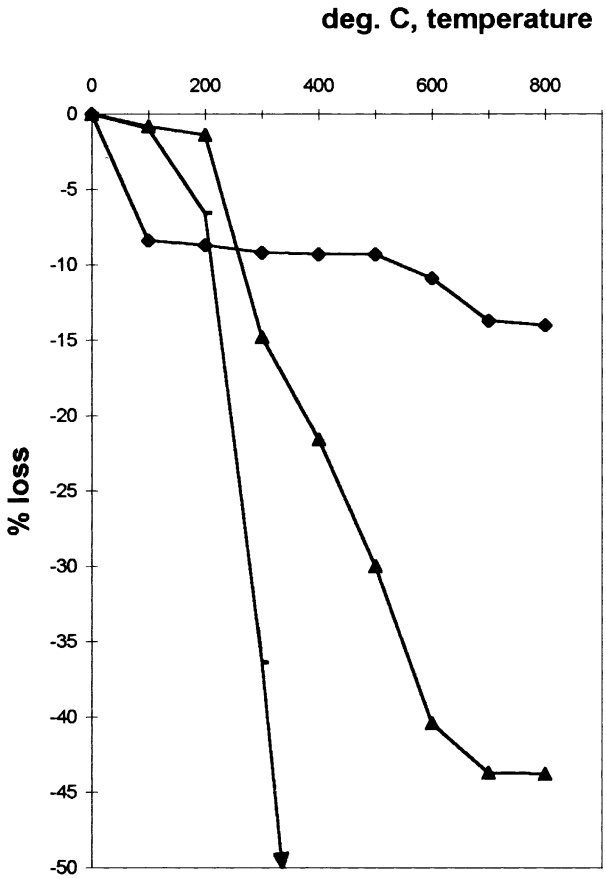

Fig. 6. Thermogravimetry (isothermal heating) of MM, free ODA and OM including ODA^+. ◆ – MM ▲ – OM (ODA^+) — – ODA°.

an ODA^+ based OM, are presented. Before heating the specimens were dried for a week at 30 °C.

As may be seen, the extra-lattice water (mostly in the gallery) content of an OM (loss at 100 °C), is much lower (~1%) than that of the pristine smectite (8–10%). The H_2O IR signal (3440 cm^{-1}) was not usable for estimation of water amount. The KBr matrix could not be fully dried and its residual water contributes to the molecular water signal. The mass loss in the 200–500 °C range is practically all related to the pyrolysis and oxidation of the organic content. At higher temperatures, contributions from both the intralattice water and the organic decomposition to the mass loss exist. As opposed to the case of free ODA (7% mass loss), the decomposition of the ODA^+, situated within the MM gallery, at 200 °C, is only in an incipient (0.5% mass loss) stage. For the bonded ODA^+ at 300 °C, the organic loss is still only 14%, becoming significant only for temperatures ⩾350 °C. Such a behavior suggests quite strong bonding between the OGP and the MM. This means that in an ODA^+-including OM the gap is expanded, compared to pristine MM, but the silicate/gallery species bonding is also strengthened compared to the situation in the pristine MM.

Interestingly, the H_g of the OMs (based on ODA^+) exposed to 250–280 °C is slightly raised, despite the loss of some of the OGP, suggesting stereo chemical modifications. Heating to 300 °C or higher provokes a steep decrease of the H_g values, which at 350 °C become similar to those of pristine MM.

3.2.3. The influence of the R_e ratio

OM synthesis, using ODA^+ as the OGP, was performed for a range of R_e values extending from 0.32–2.2. The relevant characteristics of the resulting OMs are collected in Table 4.

As may be seen, the amount of OGP inserted in the gallery increases until the R_e attains values around 1.7. Most of the OM preparation runs—when $R_e = 1.7$—produce OM having a H_g close to the upper limit indicated in Table 4. Practically all the added ODA^+ is absorbed by the MM. At higher R_e values the amount of inserted OGP remains in the 36–40% range. On the other hand, by repeating the reaction (without filtering), using a $R_e = 1.1$ value, it is possible to further raise the amount of inserted OGP and the H_g. In these subsequent stages, though, post-reaction processing (washing, filtering) becomes much more difficult than in the case of a one stage preparation, due to the excessive amounts of unreacted ODA. Reproducibility of the results is low.

The Na^+ is never totally eliminated. Practically, the cationic exchange stops for R_e values around 1.0. Despite this, ODA^+ continues to enter into the gallery (see $R_e = 1.7$ and 2.2 and 1.1×3). When significant amounts of non-exchange ODA^+ are present (e.g. multistage preparation), the amount of OGP evolving from the gallery at temperatures ⩾200 °C slightly increases.

At low R_e values, even the long ODA^+ chains seem to adopt a flat orientation, leaving the H_g of the pristine MM unchanged. Surprisingly, though, for a fairly low $R_e = 0.65$—when a substantial fraction of the Na^+ is still present in the gallery—the H_g jumps to almost ~20 Å, indicating a paraffin like arrangement.

3.3. Selection of optimal OGPs for high-gallery EOMs

One of the essential conditions, for an OM to gain EOM status, is the presence of a high gallery. The data presented above suggest that various strategies may be used for the preparation of OMs exhibiting high H_g values. The different options are compared, in this section—considering aspects like processing ease and raw materials cost—so as to allow identification of OGPs usable in case industrial scale production of EOM is envisaged.

Short ionic OGPs, either A^+ or A° type, are not efficient gallery enlargers. A° molecules, even of large size, are much less efficient OGPs than their cationic counterparts, generating more or less hydrophilic OMs, the characteristics of which vary from batch to batch. Preparation procedures including A° are also expensive. Large size (primary to quaternary salt) alkylammonium ions are, on the other hand, efficient penetrators, so that quite low R_e value reaction systems may be used. An excellent H_g (~30 Å), neat processing and highly reproducible result are obtainable if $DMDODA^+$ or $TMODA^+$ are used, but the cost of such OGPs is high. A good trade-off seems to be provided by ODA^+, which, at $R_e = 1.7$, offers a respectable H_g (up to 26 Å) at dramatically lower costs. Working at $R_e = 0.65$, further reduces costs, while giving EOMs with a somewhat less expanded gallery. The OMs including large alkylammonium ions also exhibit the necessary, for EOM states, organophilic character.

The correlation between the H_g of the EOMs and the structure and properties of composites derived from such nano-fillers (in the case of polyolefine matrices), is currently under study.

4. Conclusions

High-gallery organo-montmorillonites can be obtained by using cationic state amine molecules. Only molecules including long carbon chains are able to ensure substantial expansion of a pristine MM (Na^+) gallery. The alkylammonium ions, helped by exchange reactions with the gallery cations, exhibit higher gallery penetration abilities than neutral molecules, so they can be inserted from diluted solutions. Quaternary ammonium salts, possessing two long aliphatic "arms" generate

EOMs exhibiting a H_g ~30 Å, while ODA^+ produces, at similar R_e, 26 Å high-galleries. In the case of ODA^+, the H_g increases when R_e is raised, in the 0.35-1.7 domain. The increase is not linear. After a dramatic jump around $R_e = 0.6$, further increase is slow.

Various preparative strategies—for nano fillers—can be defined based on the data for MM/OGP interaction.

References

1. Whitesides, G. M., Mathias, J. P. and Seto, C. T., Molecular self-assembly and nanochemistry: a chemical strategy for the synthesis of nanosructures. *Science*, 1991, **254**, 1312–1319.
2. Gleiter, H., Materials with ultrafine microstructures: retrospectives and prospectives. *Nanostruct. Mater.*, 1992, **1**, 1–19.
3. Ozin, G. A., Nanochemistry: synthesis in diminishing dimensions. *Adv. Mat*, 1992, **4**, 612–649.
4. Novak, B., Hybrid nanocomposite materials—between inorganic glasses and organic polymers. *Adv. Mat.*, 1993, **5**, 422–433.
5. Brook, R. J. and Mackenzie, R. A. D., Nanocomposite materials. *Mat. World*, 1993, **1**, 27–30.
6. Ruiz-Hitzky, E., Conducting polymers intercalated in layered solids. *Adv. Mater.*, 1993, **5**, 334–340.
7. Hahn, H. and Averback, R. S., High temperature mechanical properties of nanostructured ceramics. *Nanostruct. Mater.*, 1992, **1**, 95–100.
8. Garvie, R. C., Hanmink, R. H. J. and Pascoe, R. T., Ceramics Steel? *Nature*, 1975, **258**, 703–704.
9. Partdrige, G. and Philips, S. V., A review of transparency in glass-ceramics. *Glass Tech.*, 1991, **32**, 82–90.
10. McCandelish, L. E., Kear, B. H. and Kim, B. K., Processing and properties of nanostructured WC-Co. *Nanostruct. Mater.*, 1992, **1**, 1219–1224.
11. Niihara, K. and Nakahira, A., Strengthening of oxide ceramics by SiC and Si_3N_4 dispersions. In *Proc. 3rd Int. Symp. of Ceramic Mat., Compo. for Engines*, Las Vegas NV, 27–30 November, 1989. K. J. Tennery, Ed. Am. Ceram. Soc. Pub., Westerville OH, USA, pp. 919–926.
12. Okada, A. and Usuky, A., The chemistry of polymer-clay hybrids. *Mat. Sci. Eng.*, 1995, **C3**, 109–115.
13. Mark, J. E., Ceramic reinforced polymers and polymer modified ceramics. *Polym. Eng. Sci.*, 1996, **36**, 2905–2920.
14. Ziolo, R., Giannelis, E., Weinstein, B. *et al.*, Matrix mediated synthesis of nanocryst. γ-Fe_2O_3; a new optically transparent material. *Science*, 1992, **257**, 219–222.
15. Frisch, H. and Mark, J. E., Nanocomposites prepared by threading polymer chains through zeolites, mesoporous silica or silica nanotubes. *Chem. Mater.*, 1996, **8**, 1735–1738.
16. Giannelis, E. P., A new strategy for synthesizing polymer-ceramic nanocomposites. *JOM*, 1992, **44**, 28–30.
17. Fukushima, Y. and Inagaki, S., Synthesis of an intercalated compound of montmorillonite and 6-polyamide. *J. Inclusion Phenom.*, 1987, **5**, 473–482.
18. Giannelis, E. P., Polymer layered silicate nanocomposites. *Adv. Mater.*, 1996, **8**, 29–35.
19. Kojima, Y., Usuki, A., Kawasumi, M. *et al.*, Mechanical properties of nylon 6-clay hybrid. *J. Mater. Res.*, 1993, **8**, 1185–1189.
20. Lan, T. and Pinnavaia, T. J., Clay-reinforced epoxy nanocomposites. *Chem. Mater.*, 1994, **6**, 2216–2219.
21. Hendricks, S. B., Lattice structure of clay minerals. *J. Geol*, 1942, **50**, 276–290.
22. Pinnavaia, T. J., Intercalated clay catalysts. *Science*, 1983, **220**, 365–371.
23. Jordan, J. W., Organophilic bentonites, I, swelling in organic liquids. *J. Phys. Colloid. Chem.*, 1949, **53**, 294–304.
24. Jordan, J. W., Alteration of the properties of bentonite by reaction with amines. *Mineral. Mag.*, 1949, **28**, 598–605.
25. Theng, B. K. G., *Chemistry of Clay-organic Reactions*. Wiley, New York, 1974.
26. MacEwan, D. M. C., Montmorillonite minerals. In *The X-ray Identification and Crystal Structure of Clay Minerals*, ed. G. Brown. Jarrold, Norwhich UK, 1961, pp. 149–202.
27. Grimm, R. E., *Clay Mineralogy*. McGraw Hill, NY, 1968, pp 353–403.
28. Lan, T., Kaviratna, P. D. and Pinnavaia, T. J., Mechanism of clay tactoid exfoliation in epoxy-clay nanocomposites. *Chem. Mater.*, 1995, **7**, 2144–2150.
29. LeBaron, P., Wang, Z. and Pinnavaia, T. J., Polymer-layered silicate nanocomposites: an overview. *Appl. Clay Science*, 1999, **15**, 11–29.
30. Bennett, H. and Hawley, W. C., *Methods of Silicate Analysis*. Academic Press, London, 1965.
31. Weiss, A., Organic derivatives of mica-type layer-silicates. *Angew. Chem. Int. Ed.*, 1963, **2**, 134–143.
32. McAtee, J. L., Random interstratification in organophilic bentonite. *Natl. Acad. Sci. Pub.*, 1958, **566**, 308–317.
33. Hendricks, S. B., Base-exchange of the clay mineral montmorillonite for organic cations and its dependence upon adsorption due to Van der Waals forces. *J. Phys. Chem.*, 1941, **45**, 65–81.
34. Lagalay, G., Interaction of alkylamines with different types of layered compounds. *Solid State Ionics*, 1986, **22**, 43–51.
35. Hackett, E., Manias, E. and Giannelis, E. P., Molecular dynamics simulations of organically modified layered silicates. *J. Chem. Phys.*, 1998, **108**, 7410–7415.
36. Aragon, F., Cano-Ruiz, J. and MacEwan, D. M. C., β-type interlamellar sorption complexes. *Nature*, 1959, **183**, 4662–4663.
37. Vaia, R. A. and Giannelis, E. P., Polymer melt intercalation in organically-modified layered silicates: model predictions and experiment. *Macromolecules*, 1997, **30**, 8000–8009.